Oxidation of amino acids by peracetic acid: Reaction kinetics, pathways and theoretical calculations

Penghui Du [a, b, d], Wen Liu [b, c], Hongbin Cao [a], He Zhao [a], Ching-Hua Huang [b, *]

[a] Beijing Engineering Research Center of Process Pollution Control, Division of Environment Technology and Engineering, Institute of Process Engineering, Chinese Academy of Sciences, Beijing 100190, China
[b] School of Civil and Environmental Engineering, Georgia Institute of Technology, Atlanta, GA 30332, United States
[c] The Key Laboratory of Water and Sediment Sciences, Ministry of Education, College of Environmental Science and Engineering, Peking University, Beijing 100871, China
[d] University of Chinese Academy of Sciences, Beijing 100049, China

ARTICLE INFO

ABSTRACT

Peracetic acid (PAA) is a sanitizer with increasing use in food, medical and water treatment industries. Amino acids are important components in targeted foods for PAA treatment and ubiquitous in natural waterbodies and wastewater effluents as the primary form of dissolved organic nitrogen. To better understand the possible reactions, this work investigated the reaction kinetics and transformation pathways of selected amino acids towards PAA. Experimental results demonstrated that most amino acids showed sluggish reactivity to PAA except cysteine (CYS), methionine (MET), and histidine (HIS). CYS showed the highest reactivity with a very rapid reaction rate. Reactions of MET and HIS with PAA followed second-order kinetics with rate constants of 4.6 ± 0.2, and 1.8 ± 0.1 $M^{-1} \cdot s^{-1}$ at pH 7, respectively. The reactions were faster at pH 5 and 7 than at pH 9 due to PAA speciation. Low concentrations of H_2O_2 coexistent with PAA contributed little to the oxidation of amino acids. The primary oxidation products of amino acids with PAA were [O] addition compounds on the reactive sites at thiol, thioether and imidazole groups. Theoretical calculations were applied to predict the reactivity and regioselectivity of PAA electrophilic attacks on amino acids and improved mechanistic understanding. As an oxidative disinfectant, the reaction of PAA with organics to form byproducts is inevitable; however, this study shows that PAA exhibits lower and more selective reactivity towards biomolecules such as amino acids than other common disinfectants, causing less concern of toxic disinfection byproducts. This attribute may allow greater stability and more targeted actions of PAA in various applications.

© 2018 Published by Elsevier Ltd. This is an open access article under the CC BY-NC-ND license (http://creativecommons.org/licenses/by-nc-nd/4.0/).

1. Introduction

Peracetic acid (PAA), as a wide-spectrum antimicrobial agent, has been used in water disinfection and food sanitization since early 1940s (Rossoni and Gaylarde, 2000; Kitis, 2004). Commercial PAA solution is a colorless, quaternary equilibrium mixture of PAA, hydrogen peroxide (H_2O_2), acetic acid and water according to Equation (1) below:

$$CH_3C(=O)OH + H_2O_2 \leftrightarrow CH_3C(=O)OOH + H_2O \qquad (1)$$
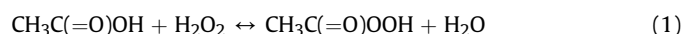
The oxidation potential of PAA (1.76 V) is close to H_2O_2 (1.80 V),

higher than aqueous chlorine (1.48 V) and chlorine dioxide (1.28 V) (Luukkonen and Pehkonen, 2017). PAA has been reported to be a more efficient disinfectant than chlorine and chlorine dioxide in inactivating pathogenic and indicator microbes (Salgot et al., 2002; Kitis, 2004; Dell'Erba et al., 2007). The advantages of PAA disinfection includes stability, low cost, and harmless disinfection byproducts (DBPs) (Dell'Erba et al., 2007; Voukkali and Zorpas, 2015). Thus, as a disinfectant or sterilant, PAA has a wide application in various industries including water treatment, food processing, medical, and textile (Kitis, 2004; Falsanisi et al., 2006). A number of pilot- or full-scale trials of using PAA as an alternative to chlorine for wastewater disinfection have been conducted in Europe and North America (Veschetti et al., 2003; Koivunen and Heinonen-Tanski, 2005; González et al., 2012; Eckert, 2013). In the U.S., the Environmental Protection Agency has authorized

---

* Corresponding author.
  E-mail address: ching-hua.huang@ce.gatech.edu (C.-H. Huang).

the use of PAA in fruits, vegetables and meat processing as well as in wastewater and storm water disinfection (EPA, 1998, 1999, 2012).

The traditional chlorine disinfection in water treatment and food production may cause the formation of various chlorinated DBPs, some of which are potentially carcinogenic (Fukayama et al., 1986). Since the increasing use of PAA, the possible reaction of organic matter with PAA and formed byproducts have drawn great attention. An earlier study reported that PAA failed to degrade several target pharmaceuticals in wastewater at low doses (Hey et al., 2012). On the other hand, Cai et al. (2017) demonstrated that the combination of PAA with UV could lead to rapid degradation of pharmaceuticals with investigation of involved reactive species. Zhang et al. (2017) showed that PAA alone could degrade several β-lactam antibiotics in surface water and wastewater relatively quickly; however, the reaction rates were much slower in comparison to those with common oxidants such as O_3, chlorine, and Fe(VI). Meanwhile, the detected transformation products of β-lactams were mostly sulfoxide products instead of mineralized compounds, indicating the modest oxidizing ability of PAA. In general, the above studies were consistent with an early research that reported PAA solution was virtually unaffected in the presence of organic matter (Rodgers et al., 2004).

Amino acids are among the primary components of dissolved organic nitrogen in the aquatic environment. They are ubiquitous in the environment at concentrations up to $10\,g{\cdot}L^{-1}$ in surface waters (Trehy et al., 1986) and higher in wastewaters. Amino acids are also widely found in meats, fruits and vegetables in the form of proteins (Wu, 2009). Thus, amino acids have a great chance to encounter disinfectants during water treatment or food processing. The transformation of amino acids in chlorination processes has been well studied, with corresponding aldehydes and nitriles as the primary byproducts as well as toxic chlorinated products such as dihaloacetonitriles and chloral hydrate (Trehy et al., 1986; Pattison and Davies, 2001). In contrast, the potential reactions between amino acids and PAA during water treatment remain unclear and have been scarcely investigated. It is important to evaluate the transformation of amino acids and whether harmful byproducts are formed during PAA reactions in order to improve the applications of PAA in water treatment.

Some previous studies indicated that the amino acid composition in blood meal or organic matter may change after PAA treatment (Schnitzer and Hindle, 1980; Kerkaert et al., 2011; Hicks et al., 2015). Schnitzer and Hindle (1980) reported that PAA treatment may decrease the amino acid-N component in humic materials. Literature also suggested that oxidation by PAA may result in increase of hydrophilicity of the proteins through crosslinking destruction, whereas hypochlorous acid oxidation commonly results in protein aggregation (Kerkaert et al., 2011; Hicks et al., 2015). Extensive literature search indicates that there has been little information regarding the reaction kinetics and mechanism of the oxidation of amino acids by PAA to date. Thus, this study was motivated to address this knowledge gap.

The specific objectives of this work were to: (1) determine the reactivities of a range of amino acids towards PAA; (2) assess the impact of background H_2O_2 and solution pH on the oxidation reaction of amino acids with PAA; and (3) elucidate the transformation products and reaction mechanism via product characterization and theoretical analysis of amino acids' reactive sites. All the experiments were conducted using PAA dosage and pH conditions relevant to those common in wastewater treatment or food processing with PAA applications.

2. Materials and methods

2.1. Chemicals

Analytical-grade L-arginine (ARG), L-histidine (HIS), L-aspartic acid (ASP), and L-glycine (GLY) were purchased from Acros Organics. Other amino acids including L-cysteine (CYS), L-proline (PRO), L-methionine (MET), L-tyrosine (TYR), and L-glutamic acid (GLU) were obtained from MP Biomedicals at >98% purity. The structures of the selected amino acids are shown in Fig. S1. PAA solution (~39% PAA, 6% H_2O_2 and ~45% acetic acid, w/w), sodium dihydrogen phosphate, disodium hydrogen phosphate, sodium thiosulfate, and sodium borohydride were purchased from Sigma Aldrich (St. Louis, MO, USA). Hydrogen peroxide solution (~30% H_2O_2 in water, w/w) was purchased from Fisher Scientific (Waltham, MA, USA). Reagent-grade deionized water ($\geq 18\,m\Omega$-cm) was generated from a Milli-Q integral water purification system (Millipore, Billerica, MA, USA) and used to prepare working solutions. The working solution of each amino acid at 10 mM was freshly prepared and used within 24 h. Fresh PAA working solutions at 100 mM were prepared every week by diluting the PAA stock. The H_2O_2 working solution was prepared at 11 mM. All stock and working solutions were stored at $4-5\,^{\circ}C$ before use.

2.2. PAA oxidation experiments

PAA oxidation experiments were conducted in 200-mL glass beakers with magnetic stirring at room temperature. Reaction solutions were maintained at desired pH using phosphate buffer (10 mM). Reactions were initiated by spiking an appropriate amount of PAA or H_2O_2 working solution into the buffered solution containing 10 μM amino acids. Aliquots were periodically taken and injected into HPLC vials containing an excess amount of sodium thiosulfate or sodium borohydride relative to the PAA concentration. The quenched samples were analyzed within 12 h after a derivatization process as described below. The reactions with H_2O_2 were conducted similarly by adding an appropriate amount of H_2O_2 working solution to the buffered reaction solution containing 10 μM selected amino acids.

2.3. Analytical methods

Titration methods were applied to determine the concentrations of PAA and H_2O_2, respectively, in the PAA stock solution as previously described (Cai et al., 2017). Iodometric titration was used to determine the combined concentration of PAA and H_2O_2, and potassium permanganate titration under acidic pH was used to determine the H_2O_2 concentration in the stock. The latter method was also used to determine the H_2O_2 concentration in pure H_2O_2 stock solution. The lower concentrations of PAA in the PAA working solution and in the oxidation experiments were quantified by the standard *N,N*-diethyl-*p*-phenylenediamine (DPD) titration method (APHA et al., 1998) as described previously (Cai et al., 2017).

The concentrations of residual amino acids in the reactions were determined using an Agilent 1100 high performance liquid chromatography (HPLC) equipped with a fluorescence detector after derivatization (detailed in Supporting Information (SI) Text S1). Monobromobimane (mBBr) was used as a derivatization reagent for CYS determination, while *o*-phthalaldehyde (OPA) was used for the other amino acids. After derivatization, 20 μL of sample was separated on an Agilent Zorbax SB-C18 column (2.1 × 150 mm, 5 μm) with a flow rate of 0.3 mL/min. The mobile phase was a mixture of (A) sodium acetate buffer (5 mM) at pH 5.9, and (B) acetonitrile. The eluent composition changed linearly from initially 10% A to 50% at 7 min and then was so maintained for 3 min,

followed by re-equilibration to the starting condition. The excitation and emission wavelengths for fluorescence detection were set respectively at 395 and 475 nm for the mBBr derivatization method, and 340 and 455 nm for the OPA derivatization method.

The oxidation products of selected amino acids by PAA were analyzed using an Agilent 1100 Series LC/MSD system equipped with an Agilent Zorbax SB-C18 column (2.1 × 150 mm, 5 μm) with a flow rate at 0.3 mL/min. The mobile phase consisted of (A) deionized water with formic acid (0.1%, v/v), and (B) methanol. The gradient of the mobile phase B was kept at 5% in the first 5 min, then ramped to 90% at 10 min and maintained for 3 min, and then re-equilibrated to the starting condition. The injection volume was 10 μL. The mass spectrometer was set at negative electrospray ionization mode (ESI-) with a 70 V fragmentation voltage and 4000 V capillary voltage. Nitrogen was used both as the drying gas at 350 °C (6.0 L/min) and nebulizer gas (25 psi). A full-scan mode from 50 to 500 m/z was applied to examine the transformation products.

2.4. Computational method

All calculations were performed using Gaussian 03 software (Frisch et al., 2003). Geometry optimization calculations were executed without any constraints using the B3LYP method with 6-31G(d,p) basis set (Hariharan and Pople, 1973; Lee et al., 1988; Becke, 1993; Raghavachari, 2000). Condensed Fukui function (CFF), an important concept in conceptual density functional theory, was computed based on natural population analysis (NPA) charge to predict the regioselectivity of the oxidation of amino acids by PAA (Parr and Yang, 1984; Olah et al., 2002). All of the above calculations were performed in the gas phase.

3. Results and discussion

3.1. Evaluation of PAA reactivity to different amino acids

To assess the possible reaction between amino acids and PAA, a total of nine essential amino acids, which were widely detected in vegetables, fruits, and meats, were selected to study their reactivity towards PAA oxidation. As shown in Fig. 1, most amino acids are sluggish to PAA oxidation except CYS, MET and HIS. CYS was completely oxidized by PAA in 30 min, suggesting its high reactivity towards PAA oxidation. The high reactivity of CYS may be caused by its thiol group, which could be easily oxidized to its disulfide form (RS–SR) (Nakamoto and Bardwell, 2004; Rehder and Borges, 2010). MET and HIS were also observed with >25% transformation under the same condition. This is consistent with an early study that reported the sulfur-containing amino acids in meat would greatly decreased after PAA treatment, while most of the other amino acids showed little changes (Hicks et al., 2015). Unlike PAA treatment, chlorination was found with high reactivity towards all amino acids. The presence of amino acids during chlorination processes may greatly reduce the disinfection efficiency and produce DBPs such as trihalomethanes and halonitriles, which may have adverse effects on human health (Na and Olson, 2007). On the basis that the amounts of HIS, CYS, and MET in fruits and vegetables are typically low (Brückner and Westhauser, 2003) and the low reactivities of other amino acids to PAA, PAA oxidation probably will not change the organic composition of the treated food or wastewater significantly and much less byproducts would be formed, in comparison with other common oxidants such as chlorine.

3.2. Reaction kinetics of selected amino acids with PAA

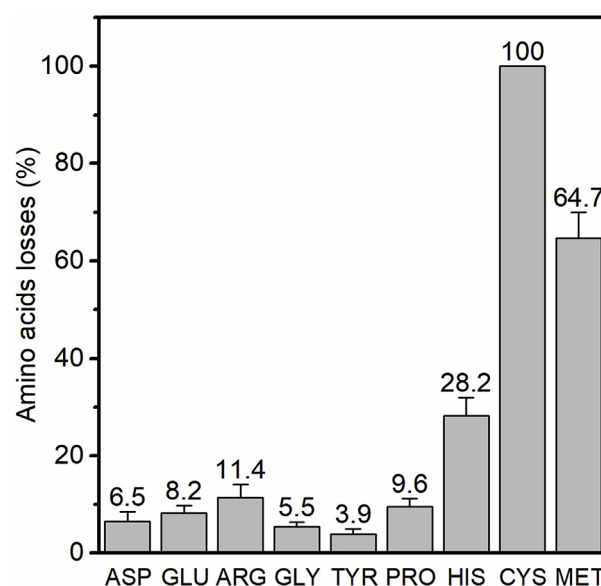Owing to their higher reactivity, CYS, MET and HIS were selected

Fig. 1. Losses of nine selected amino acids by PAA (Amino acids: 10 μM, PAA: 131 μM, incubation time: 30 min; room temperature). The order of nine amino acids in Fig. 1 is set based on their amounts in strawberry samples (from highest to lowest) (Gebhardt et al., 2008). Error bars represent standard deviation from duplicate samples.

to further study their reaction kinetics with PAA. Notably, under the employed reaction conditions ($[CYS]_0 = 10$ μM, $[PAA]_0 = 131$ μM (i.e., 10 ppm), pH = 7.0), CYS was completely oxidized by PAA within 1 min. The reaction was too fast to quantify the rate constant using the batch reactor set-up. The reactions of MET and HIS with PAA were not as rapid and followed first-order kinetics with respect to the amino acid concentration (Fig. S2a). In addition, the pseudo-first-order rate constant (k_{obs}, min^{-1}) was found to increase linearly with PAA concentration (131–1310 μM) (Fig. S2b). Hence, the oxidation of amino acids by PAA can be expressed by the second-order kinetics (see Equations (2) and (3)), with the apparent second-order rate constant (k_{app}, M^{-1}·s^{-1}) obtained by dividing the k_{obs} value by the PAA concentration.

$$\frac{d[\text{Amino acid}]}{dt} = -k_{obs}[\text{Amino acid}] \tag{2}$$

$$\frac{d[\text{Amino acid}]}{dt} = -k_{app}[\text{PAA}][\text{Amino acid}] \tag{3}$$

where k_{obs} is the observed first-order rate constant, k_{app} is the apparent second-order rate constant for the overall reaction, [Amino acid] and [PAA] are the concentration of amino acid and PAA, respectively.

The k_{app} values for MET and HIS with PAA were determined to be 4.6 ± 0.2, and 1.8 ± 0.1 M^{-1}·s^{-1}, respectively. To be noted, the k_{app} value for CYS towards PAA should be much larger, at least greater than 5.8 × 10^2 M^{-1}·s^{-1}, which is near the upper limit that could be measured by the batch reaction set-up in this study. The difference in k_{app} among amino acids towards PAA is likely caused by the side chain groups, which will be fully discussed later based on the products identification and reactive sites evaluation. Meanwhile, Table 1 indicates that the reaction rates of amino acids with other common oxidants are usually several orders of magnitude higher than those with PAA. This is similar to our earlier study that showed PAA has a slower reaction rate towards β-lactam antibiotics than other water treatment oxidants (Zhang et al., 2017). As a promising disinfectant, PAA shows limited ability to degrade organic

Table 1
Values for the second-order reaction rate constants ($M^{-1} \cdot s^{-1}$) for CYS, MET, and HIS with chemical oxidants at pH 7.0–7.4.[a]

	HOCl	HBrO	O_3	PAA
CYS	3.0×10^7	1.2×10^7	4.4×10^9	$>5.8 \times 10^2$
MET	3.8×10^7	3.6×10^6	4.0×10^6	4.6
HIS	1.0×10^5	3.0×10^6	5.3×10^6	1.8

[a] Rate constants were from experiments in this study for PAA (pH 7.0) and from literature (Pryor et al., 1984; Pattison and Davies, 2001, 2004) for HClO, HBrO, and O_3 (pH 7.4).

biomolecules and micropollutants. This attribute may be beneficial for the further application of PAA in various industries, as PAA will not be easily consumed by organic matter in water and will not generate chlorinated DBPs or other harmful byproducts commonly formed from chlorine disinfection (Acero et al., 2010).

3.3. Effect of H_2O_2 on oxidation of amino acids by PAA

H_2O_2 is an important component in commercial PAA solutions; however, the role of H_2O_2 in the oxidation of amino acids by PAA solutions is unknown. In this work, CYS, MET and HIS were reacted with H_2O_2 only to study the impact of H_2O_2 on amino acids oxidation. It was found that the concentration of background H_2O_2 (about 33 μM) in the PAA solution was too low to cause any significant transformation of amino acids at pH 7. Thus, the concentration of H_2O_2 was increased to 131 μM (the same as the PAA concentration, as some commercial PAA solutions may have a lower PAA/H_2O_2 molar ratio (Shah et al., 2015)) in order to assess the reaction kinetics. Fig. 2 shows that 131 μM of H_2O_2 could only oxidize 15% of CYS, 5.5% of MET, and 3.4% of HIS in 30 min. Meanwhile, under the same concentration of PAA, PAA could oxidize 100%, 65%, and 28% of the amino acids, respectively. The second-order rate constants of CYS and MET with H_2O_2 at pH 7 were about 5.7×10^{-1} and $8.9 \times 10^{-2}\,M^{-1} \cdot s^{-1}$, respectively. These kinetic results are comparable to the earlier research that have calculated the second-order rate constants of CYS and MET in the oxidation by H_2O_2 to be around $2.7 \times 10^{-1}\,M^{-1} \cdot s^{-1}$ (pH 5.7) and

1.6×10^{-2} (pH 5.5–6.0), respectively (Boonvisut et al., 1982; Chu et al., 2016). Evidently, the oxidation of amino acids by H_2O_2 is much slower than that by PAA, indicating that PAA is the primary oxidant in PAA solution dominating the transformation of amino acids. This finding is consistent with our previous study that it was PAA, not H_2O_2, that induced the oxidation reaction of β-lactams, and there was no obvious synergistic or inhibitory effect between PAA and H_2O_2 (Zhang et al., 2017). Earlier literature also has concluded that the antimicrobial effect of PAA is far greater than H_2O_2 (Lubello et al., 2002; Kitis, 2004). Thus, in the applications of PAA solutions, it is mainly PAA that is responsible for antibacterial and compound oxidation.

### 3.4. Effect of pH on PAA oxidation of amino acids

PAA and amino acids are both ionizable compounds. The primary species of PAA and amino acids under different pH conditions may vary according to the acid dissociation constants, which may cause different reaction behaviors in the oxidation of amino acids by PAA. As shown in Fig. 3, the pseudo first-order rate constants of MET and HIS by PAA oxidation at pH 5 and 7 were comparable, but decreased significantly at pH 9.

The pKa of PAA is around 8.2 (Luukkonen and Pehkonen, 2017) and the acid-base dissociation could result in varied distribution of neutral (PAAH) and charged (PAA$^-$) species. According to the speciation, neutral PAAH is dominant (over 94%) at pH 5 and 7, while anionic PAA$^-$ becomes dominant (over 89%) at pH 9. Speciation of amino acids may be another factor. For MET and HIS, the acidity constants of the carboxylic acid group on the α-carbon are 2.28 and 1.82, and the acidity constants of the protonated α-amino group are 9.21, and 9.17, respectively. HIS has an additional acidity constant for its imidazole ring –NH at 6.00 (Linde, 1991). The species distributions of PAA, MET and HIS at pH 5, 7, and 9 are depicted in Table S1 and Fig. S3.

From pH 5 to 7, the amount (99.9–92.1%) of PAAH changed little and could explain why the rate constants were comparable at pH 5 and 7 as it was PAAH having the strong oxidizing ability rather than PAA$^-$ (Zhang et al., 2017). At pH 9, the lower distribution (10.4%) of PAAH could lead to the lower rate constants for oxidation of amino
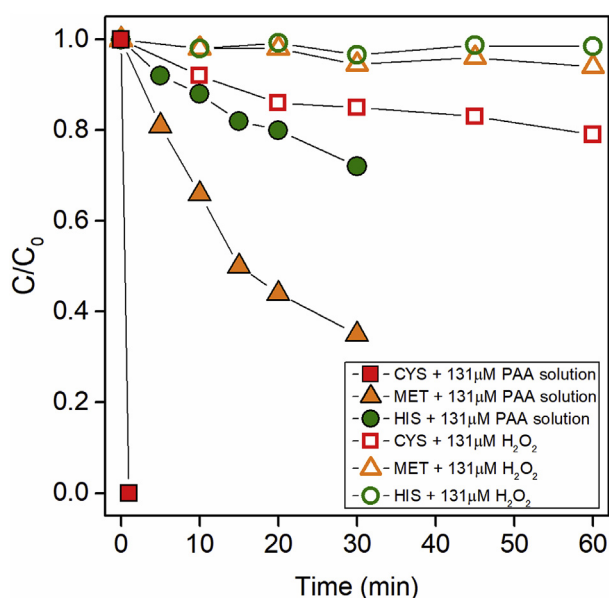
Fig. 2. Time course of transformation of CYS, MET, and HIS with PAA solution (solid dots) and H_2O_2 solution (valid dots). Experimental conditions: [amino acids]$_0$ = 10 μM, [PAA]$_0$ = 131 μM, [H_2O_2]$_0$ = 131 μM, pH = 7, room temperature.
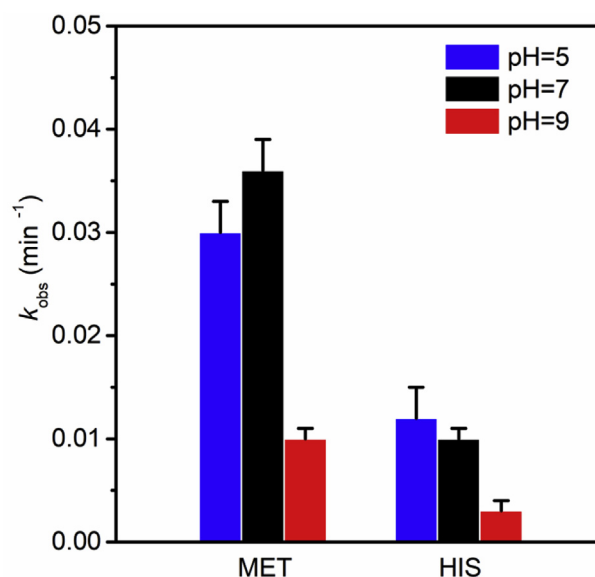
Fig. 3. Pseudo first-order rate constants of MET, and HIS with PAA at different pHs. [amino acids]$_0$ = 10 μM, [PAA]$_0$ = 131 μM, room temperature.

acids. For amino acids' speciation, MET had the same neutral, zwitterion species dominant at pH 5 and 7, while HIS's imidazole −NH group changed from being protonated to non-protonated from pH 5 to 7 (Fig. S3). The very similar rate constants of HIS at pH 5 and 7 suggest that the impact of HIS species on HIS oxidation by PAAH was negligible. Thus, it can be concluded that the rate constants for PAA oxidation are lower at alkaline solution due to the lower distribution of PAAH species, while the speciation of the targeted amino acids have much less influence on the reaction rate.

3.5. Reaction products and pathways

The transformation products of CYS, MET, and HIS by PAA oxidation were assessed and the results are presented in Table 2, with proposed transformation pathways in Fig. 4. The MS results showed that disulfide (CYS dimer), sulfinic acid (CYSO$_2$H), and sulfonic acid (CYSO$_3$H) were the three major products of oxidation of CYS by PAA. The formation of CYSOH was not detected, which was likely due to its high instability (Penn et al., 1978). The above compounds are well-known CYS oxidation products (2M-1, M+16, M+32, and M+48, where M = molecular weight of parent CYS) under various conditions because of the reactive thiol functional group (Milne and Zika, 1993; Greer et al., 1996; Hawkins and Davies, 2001; Mailloux et al., 2014). In this study, PAA likely attacks the highly nucleophilic thiol group, which may result in formation of CYSOH. Compounds with the −SOH group were found to be extremely difficult to detect and quantify due to the much lower pKa than that of the −SH group (Enami et al., 2009; Hugo et al., 2009; McGrath et al., 2010). CYSOH may couple with another CYS to form the CYS dimer through intermolecular disulfide bridging. CYSOH can also undergo further oxidation to generate CYSO$_2$H and CYSO$_3$H (Fig. 4a).

Ion chromatography was employed to determine whether oxidation of CYS by PAA could generate small ions. The results suggested that CYSO$_3$H was the final product as only a new peak of CYSO$_3$$^-$ emerged at 12.9 min, while no SO$_4$$^{2-}$ (standard R.T. = 11.2 min) or other small organic carboxylic acids were detected (Fig. S4). This is rather different from other chemical oxidants, such as O$_3$ or HClO, which were able to break bonds and finally form ions including aliphatic acids, SO$_4^{2-}$, and/or NO$_3^-$ (Mudd et al., 1969; Wenk et al., 2013).

The reaction pathway for MET oxidation by PAA is rather simple that MET was expected to be oxidized to generate the M+16 intermediate (i.e. MET sulfoxide) (Fig. 4b). Previous research also observed MET sulfoxide as the primary product during oxidation of MET by H$_2$O$_2$ (Keck, 1996). MET sulfoxide is believed to contribute to biological aging as it increases with age in body tissues. Oxidation of MET may cause the accumulation of damaged, nonfunctional proteins (Shringarpure and Davies, 2002; Stadtman et al.,

2005).

The M+32 (m/z 186) is the predominant intermediate (based on peak area) of HIS oxidation by PAA, while the dimeric product (m/z 323) may be formed via nucleophilic addition of m/z 186 by another HIS at the C9 site followed by loss of a water (Fig. 4c). Similar reaction products were also detected in the oxidation of HIS by ^{1}O$_2$, •OH, or in other oxidation systems (Tomita et al., 1969; Agon et al., 2006; Amano et al., 2014; Liu et al., 2014).

Based on the results above, it can be concluded that PAA is a weak oxidant that the corresponding oxidation products are mostly substrates with one or more [O] addition, which is consistent with previous observations (Zhang et al., 2017). The thiol group of CYS was oxidized to sulfinic and sulfonic acids, as well as to generate CYS dimers. The thioether sulfur of MET is oxidized to sulfoxide by PAA. [O] addition on the imidazole ring was also demonstrated to be the primary reaction pathway for HIS oxidation by PAA. Moreover, PAA appears to be only reactive to organics with specific functional groups, such as thiol, thioether sulfur, as well as specific groups with high electron distribution.

3.6. Theoretical prediction of reactive sites on selected amino acids

PAA is a well-known electrophilic oxidant, as the molecular orbitals shown in Fig. S5 well demonstrates the electron-deficient property around the peroxyl group of PAA. According to the products identified and general oxidation reaction mechanism, PAA is likely to accept electrons from amino acids and give out an oxygen atom. The condensed Fukui function (CFF), commonly used in prediction of reactive sites of electrophilic, nucleophilic, and radical attacks (Parr and Yang, 1984), was used to predict the reactive sites on selected amino acids towards PAA attacks. The detailed description for the CFF concept and the calculation method are presented in Text S2.

As presented in Fig. 5, the ability of losing electron was quantified and visualized on every site of amino acids by the calculated Fukui index (f_k^-). The f_k^- on sulfur atom in CYS and MET is much higher than that on the other sites, suggesting the strong affinity of sulfur-containing organics towards PAA oxidation, which is in accordance with the fact that most of the known organic compounds that react fast with PAA are those with sulfur atom(s) (Chipiso et al., 2016; Zhang et al., 2017). Moreover, the corresponding products are mostly sulfoxides and other following products. Meanwhile, the f_k^- distribution on HIS molecule is less differential, with values of 0.103, 0.095, 0.116, and 0.148 at C1, C5, C7, and C9, respectively. Thus, the oxygen atom from PAA likely prefers addition onto C9 or C7 of HIS as we proposed in Fig. 4c. Then, the [O] addition intermediate coupled with another HIS molecule and formed a dimer product. Based on the products identified and theoretical calculations, we proposed that the sites with higher CFF values are more likely to be attacked by PAA, forming corresponding [O] addition products and other derivatives.

Since the PAA-induced direct oxidation was considered to be electrophilic attacks, the reactivity of amino acids towards PAA oxidation is likely related to their nucleophilicities. Thus for the comparison of different amino acids, the nucleophilicity index was used, which measures the energy stabilization when an optimal electronic charge transfer from the system to the environment occurs (De Vleeschouwer et al., 2007). To describe the nucleophilic character of a reactive site within a molecule, a local nucleophilicity index N_k can be proposed:

$$N_k = Nf_k^- \tag{4}$$

where N is the global nucleophilic index, which is calculated based

Table 2
MS identified products of CYS, MET, and HIS with PAA oxidation.[a]

	m/z	Molecular weight	Retention time (min)	Peak Area[b] ($\times 10^5$)
CYS	120	121(M)	1.60	—
	152	M+32	1.69	0.06
	168	M+48	1.56	0.56
	239	2M −1	1.58	0.15
MET	148	149 (M)	2.31	1.66
	164	M+16	1.69	0.71
HIS	154	155 (M)	2.20	4.00
	186	M+32	2.12	4.76

[a] Initial concentration of amino acids and PAA were 10 and 131 μM, respectively.
[b] Peak area values for amino acids and corresponding products at 1 min for CYS, 30 min for MET and HIS.
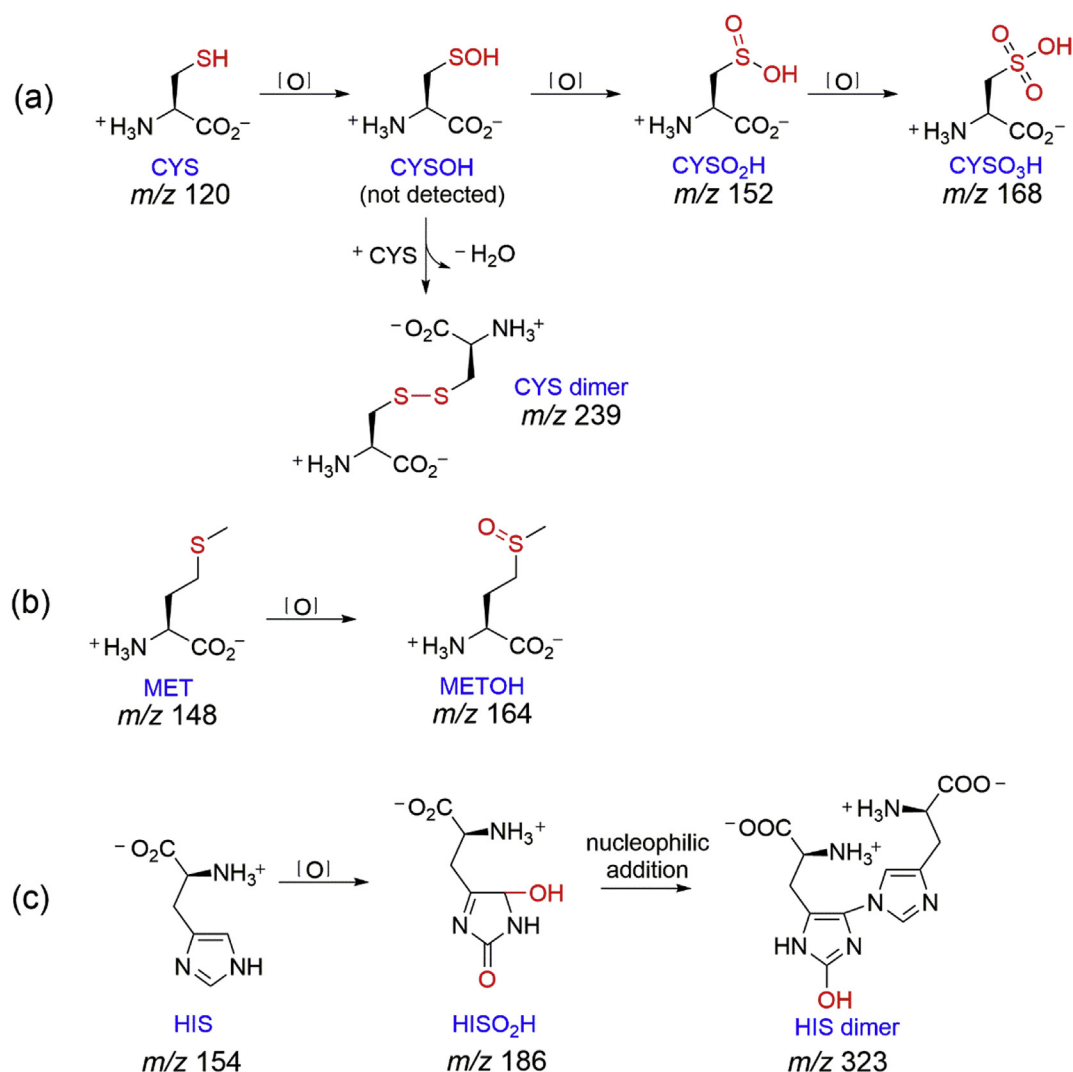
Fig. 4. Proposed reaction pathways for (a) CYS, (b) MET, and (c) HIS oxidation by PAA.
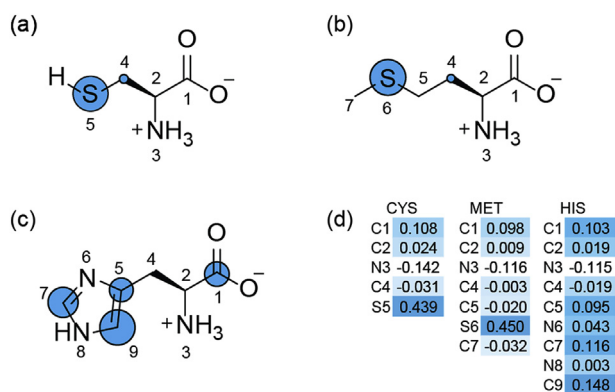

Fig. 5. Visualized Fukui index (f_k^-) on selected amino acids by electrophilic PAA attacks. (a) CYS, (b) MET, (c) HIS, (d) Fukui electrophilic attack index (f_k^-) distribution data. The diameters of blue circles represent relative f_k^- values on the specific site.

on the electronic chemical potential μ and chemical hardness η (see SI Text S3); and f_k^- displays its maximum value, i.e. at the active site (k) of the nucleophile.

Note that the local nucleophilicity index contains a global

contribution N as a factor of the genuine local nucleophilic index f_k^-. Table 3 summarizes the values of electrostatic descriptors, including the global and local nucleophilicity indexes, for 12 amino acids. CYS shows the S5 sulfur atom as the preferential site for electrophilic attack on the basis of the Fukui function, $f_k^- = 0.439$, and the local nucleophilicity, $N_k = 0.850$ eV. MET presents a local nucleophilicity value of $N_k = 0.768$ eV at sulfur atom S6. Note that HIS, having multiple reactive sites due to the close Fukui function values at C7 and C9, presents a local nucleophilicity value of $N_k = 0.653$ eV with the sum of two reactive sites. The local nucleophilicity index of CYS, MET and HIS are much higher than those of the other amino acids, suggesting that they are easier to undergo electrophilic attacks on the specific sites. This is consistent with our experimental results that CYS, MET and HIS were oxidized more easily than the other amino acids by PAA (Fig. 1). Moreover, the N_k values of three more amino acids (leucine (LEU), threonine (THR), and tryptophan (TRP)) with typical alkyl, hydroxyl and indole side chains were also calculated, and their reactivities towards PAA oxidation can thus be predicted. The results in Table 3 indicate that LEU and THR may show less reactivity, while TRP could be a potential substrate for PAA oxidation due to its side chain indole. According to our work and published literature, compounds containing sulfur atoms or rings with nitrogen atoms are always found

Table 3
Electrostatic descriptors for 12 amino acids at B3LYP/6-31g(d,p) level. The units for these descriptors are all eV except f_k^-.

Amino acids	Electron affinity (A)	Ionization potential (I)	Electronic chemical potential (μ)	Chemical hardness (η)	Global nucleophilicity index (N)	f_k^-	Local nucleophilicity index (N_k)
ARG	−1.338	8.048	−3.355	9.386	1.668	0.271	0.452
ASP	−2.208	9.228	−3.510	11.437	1.856	0.110	0.204
CYS	−2.130	8.874	−3.372	11.004	1.936	0.439	0.850
GLU	−1.880	9.114	−3.617	10.995	1.681	0.105	0.176
GLY	−2.846	9.478	−3.316	12.324	2.242	0.161	0.361
HIS	−2.330	8.060	−2.865	10.390	2.532	0.258[a]	0.653
MET	−1.417	8.089	−3.336	9.506	1.708	0.450	0.768
PRO	−2.717	8.460	−2.872	11.177	2.710	0.125	0.339
TYR	−1.636	7.855	−3.110	9.491	1.963	0.152	0.298
LEU	−2.728	9.282	−3.277	12.009	2.237	0.121	0.271
THR	−2.639	9.341	−3.351	11.980	2.133	0.118	0.252
TRP	−1.269	7.577	−3.154	8.846	1.778	0.285[a]	0.507

[a] The sum of the largest two f_k^- values was applied due to the wide distribution of reactive sites on HIS molecule.

to be highly nucleophilic, and more likely to undergo PAA oxidation (Chipiso et al., 2016; Zhang et al., 2017). However, descriptor N_k could only qualitatively predict the reactivities of amino acids, and more parameters and factors should be considered to establish a better model.

4. Conclusions

This work demonstrates that PAA has low reactivity with amino acids except those with reactive side chains including thiol group (CYS), thioether group (MET), and imidazole ring (HIS). The background H_2O_2 in the PAA solution has a negligible effect on the reactions of amino acids with PAA. PAA oxidation of MET and HIS is much slower at pH 9 than at pH 5 and 7 due to the speciation of PAA. The combined results from experimental measurements and theoretical calculations show that PAA is prone to attack amino acids with strong nucleophilicity, delivering [O] to the electron-rich sites. Overall, it can be concluded that the widely used PAA solution is much less reactive towards organics than other common disinfectants, thus resulting in longer stability and fewer byproducts formation. Moreover, PAA treatment primarily generates [O] addition products which are less harmful compared to other DBPs of concerns commonly found with disinfection oxidants such as chlorine. From the perspective of disinfectant stability and DBPs formation, the results of this study suggest that PAA is a more stable and safer oxidant, which could be suitable in food processing, wastewater treatment as well as other industries in the future.

Conflict of interest

The authors declare no conflict of interest.

Acknowledgements

Appendix A. Supplementary data

Supplementary data to this article can be found online at https://doi.org/10.1016/j.wroa.2018.09.002.

References

Acero, J.L., Benitez, F.J., Real, F.J., Roldan, G., 2010. Kinetics of aqueous chlorination of some pharmaceuticals and their elimination from water matrices. Water Res. 44 (14), 4158–4170.

Agon, V.V., Bubb, W.A., Wright, A., Hawkins, C.L., Davies, M.J., 2006. Sensitizer-mediated photooxidation of histidine residues: evidence for the formation of reactive side-chain peroxides. Free Radical Biol. Med. 40 (4), 698–710.

Amano, M., Kobayashi, N., Yabuta, M., Uchiyama, S., Fukui, K., 2014. Detection of histidine oxidation in a monoclonal immunoglobulin gamma (IgG) 1 antibody. Anal. Chem. 86 (15), 7536–7543.

APHA, AWWA, WEF, 1998. Standard methods for the examination of water and wastewater, 20th ed. American Public Health Association/American Water Works Association/Water Environment Federation, Washington, DC.

Becke, A.D., 1993. A new mixing of Hartree-Fock and local density-functional theories. J. Chem. Phys. 98 (2), 1372–1377.

Boonvisut, S., Aksnes, A., Njaa, L.R., 1982. Oxidation of methionine. Effects of hydrogen peroxide alone and in combination with iodide and selenite. Food Chem. 9 (3), 183–194.

Brückner, H., Westhauser, T., 2003. Chromatographic determination of L-and D-amino acids in plants. Amino Acids 24 (1–2), 43–55.

Cai, M., Sun, P., Zhang, L., Huang, C.-H., 2017. Uv/peracetic acid for degradation of pharmaceuticals and reactive species evaluation. Environ. Sci. Technol. 51 (24), 14217–14224.

Chipiso, K., Logan, I.E., Eskew, M.W., Omondi, B., Simoyi, R.H., 2016. Kinetics and mechanism of bioactivation via s-oxygenation of anti-tubercular agent ethionamide by peracetic acid. J. Phys. Chem. 120 (41), 8056–8064.

Chu, C.H., Erickson, P.R., Lundeen, R.A., Stamatelatos, D., Alaimo, P.J., Latch, D.E., McNeill, K., 2016. Photochemical and nonphotochemical transformations of cysteine with dissolved organic matter. Environ. Sci. Technol. 50 (12), 6363–6373.

De Vleeschouwer, F., Van Speybroeck, V., Waroquier, M., Geerlings, P., De Proft, F., 2007. Electrophilicity and nucleophilicity index for radicals. Org. Lett. 9 (14), 2721–2724.

Dell'Erba, A., Falsanisi, D., Liberti, L., Notarnicola, M., Santoroa, D., 2007. Disinfection by-products formation during wastewater disinfection with peracetic acid. Desalination 215 (1–3), 177–186.

Eckert, K., 2013. Disinfection Performance of Peracetic Acid in Florida Wastewater Reuse Applications. M.S. Thesis. School of Engineering, University of North Florida.

Enami, S., Hoffmann, M.R., Colussi, A.J., 2009. Simultaneous detection of cysteine sulfenate, sulfinate, and sulfonate during cysteine interfacial ozonolysis. J. Phys. Chem. B 113 (28), 9356–9358.

EPA, 1998. National Primary Water Regulation: Disinfectants and Disinfection by products. 63 FR 69390, Washington, DC.

EPA, 1999. Combined Sewer Overflow Technology Fact Sheet. Chlorine Disinfection. EPA 832-F-99-034. Office of Water, Washington, DC.

EPA, 2012. Alternative Disinfection Methods Fact Sheet: Peracetic Acid. EPA 832-F-12-030. Office of Wastewater Management, Washington, DC.

Falsanisi, D., Gehr, R., Santoro, D., Dell'Erba, A., Notarnicola, M., Liberti, L., 2006. Kinetics of PAA demand and its implications on disinfection of wastewaters. Water Qual. Res. J. Can. 41 (4), 398–409.

Frisch, M.J., Trucks, G.W., Schlegel, H.B., Scuseria, G.E., Robb, M.A., Cheeseman, J.R., Montgomery, J.A., Vreven, T., Kudin, K.N., Burant, J.C., Millam, J.M., Iyengar, S.S., Tomasi, J., Barone, V., Mennucci, B., Cossi, M., Scalmani, G., Rega, N., Petersson, G.A., Nakatsuji, H., Hada, M., Ehara, M., Toyota, K., Fukuda, R., Hasegawa, J., Ishida, M., Nakajima, T., Honda, Y., Kitao, O., Nakai, H., Klene, M., Li, X., Knox, J.E., Hratchian, H.P., Cross, J.B., Bakken, V., Adamo, C., Jaramillo, J., Gomperts, R., Stratmann, R.E., Yazyev, O., Austin, A.J., Cammi, R., Pomelli, C., Ochterski, J.W., Ayala, P.Y., Morokuma, K., Voth, G.A., Salvador, P., Dannenberg, J.J., Zakrzewski, V.G., Dapprich, S., Daniels, A.D., Strain, M.C., Farkas, O., Malick, D.K., Rabuck, A.D., Raghavachari, K., Foresman, J.B., Ortiz, J.V.,

Cui, Q., Baboul, A.G., Clifford, S., Cioslowski, J., Stefanov, B.B., Liu, G., Liashenko, A., Piskorz, P., Komaromi, I., Martin, R.L., Fox, D.J., Keith, T., Laham, A., Peng, C.Y., Nanayakkara, A., Challacombe, M., Gill, P.M.W., Johnson, B., Chen, W., Wong, M.W., Gonzalez, C., Pople, J.A., 2003. Gaussian 03, Revision c.02.

Fukayama, M.Y., Tan, H., Wheeler, W.B., Wei, C.I., 1986. Reactions of aqueous chlorine and chlorine dioxide with model food compounds. Environ. Health Perspect. 69, 267–274.

Gebhardt, S., Lemar, L., Haytowitz, D., Pehrsson, P., Nickle, M., Showell, B., Thomas, R., Exler, J., Holden, J., 2008. USDA National Nutrient Database for Standard Reference, Release 21. United States Department of Agriculture Agricultural Research Service.

González, A., Gehr, R., Vaca, M., López, R., 2012. Disinfection of an advanced primary effluent with peracetic acid and ultraviolet combined treatment: a continuous-flow pilot plant study. Water Environ. Res. 84 (3), 247–253.

Greer, A., Jensen, F., Clennan, E.L., 1996. Ring strain effects on the interconversion of intermediates in the reaction of organic sulfides with singlet oxygen. J. Org. Chem. 61 (12), 4107–4110.

Hariharan, P.C., Pople, J.A., 1973. The influence of polarization functions on molecular orbital hydrogenation energies. Theor. Chim. Acta 28 (3), 213–222.

Hawkins, C.L., Davies, M.J., 2001. Generation and propagation of radical reactions on proteins. Biochim. Biophys. Acta Bioenerg. 1504 (2), 196–219.

Hey, G., Ledin, A., Jansen, J.l.C., Andersen, H.R., 2012. Removal of pharmaceuticals in biologically treated wastewater by chlorine dioxide or peracetic acid. Environ. Technol. 33 (9), 1041–1047.

Hicks, T.M., Verbeek, C.J.R., Lay, M.C., Manley-Harris, M., 2015. Changes to amino acid composition of bloodmeal after chemical oxidation. RSC Adv. 5 (81), 66451–66463.

Hugo, M., Turell, L., Manta, B., Botti, H., Monteiro, G., Netto, L.E.S., Alvarez, B., Radi, R., Trujillo, M., 2009. Thiol and sulfenic acid oxidation of AhpE, the one-cysteine peroxiredoxin from Mycobacterium tuberculosis: kinetics, acidity constants, and conformational dynamics. Biochemistry 48 (40), 9416–9426.

Keck, R.G., 1996. The use of t-butyl hydroperoxide as a probe for methionine oxidation in proteins. Anal. Biochem. 236 (1), 56–62.

Kerkaert, B., Mestdagh, F., Cucu, T., Aedo, P.R., Ling, S.Y., De Meulenaer, B., 2011. Hypochlorous and peracetic acid induced oxidation of dairy proteins. J. Agric. Food Chem. 59 (3), 907–914.

Kitis, M., 2004. Disinfection of wastewater with peracetic acid: a review. Environ. Int. 30 (1), 47–55.

Koivunen, J., Heinonen-Tanski, H., 2005. Peracetic acid (PAA) disinfection of primary, secondary and tertiary treated municipal wastewaters. Water Res. 39 (18), 4445–4453.

Lee, C., Yang, W., Parr, R.G., 1988. Development of the Colle-Salvetti correlation-energy formula into a functional of the electron density. Phys. Rev. B 37 (2), 785–789.

Linde, D., 1991. Handbook of Chemistry and Physics. CRC Press, Boca Raton, Ann Arbor, Boston.

Liu, F., Lu, W., Fang, Y., Liu, J., 2014. Evolution of oxidation dynamics of histidine: non-reactivity in the gas phase, peroxides in hydrated clusters, and ph dependence in solution. Phys. Chem. Chem. Phys. 16 (40), 22179–22191.

Lubello, C., Caretti, C., Gori, R., 2002. Comparison between PAA/UV and H_2O_2/UV disinfection for wastewater reuse. Water Sci. Technol. Water Supply 2 (1), 205–212.

Luukkonen, T., Pehkonen, S.O., 2017. Peracids in water treatment: a critical review. Crit. Rev. Environ. Sci. Technol. 47 (1), 1–39.

Mailloux, R.J., Jin, X., Willmore, W.G., 2014. Redox regulation of mitochondrial function with emphasis on cysteine oxidation reactions. Redox Bio. 2 (Suppl. C), 123–139.

McGrath, A.J., Garrett, G.E., Valgimigli, L., Pratt, D.A., 2010. The redox chemistry of sulfenic acids. J. Am. Chem. Soc. 132 (47), 16759–16761.

Milne, P.J., Zika, R.G., 1993. Amino acid nitrogen in atmospheric aerosols: occurrence, sources and photochemical modification. J. Atmos. Chem. 16 (4), 361–398.

Mudd, J., Leavitt, R., Ongun, A., McManus, T., 1969. Reaction of ozone with amino acids and proteins. Atmos. Environ. 3 (6), 669–681.

Na, C., Olson, T.M., 2007. Relative reactivity of amino acids with chlorine in mixtures. Environ. Sci. Technol. 41 (9), 3220–3225.

Nakamoto, H., Bardwell, J.C.A., 2004. Catalysis of disulfide bond formation and isomerization in the Escherichia coli periplasm. Biochim. Biophys. Acta Mol. Cell Res. 1694 (1), 111–119.

Olah, J., Van Alsenoy, C., Sannigrahi, A.B., 2002. Condensed Fukui functions derived from stockholder charges: assessment of their performance as local reactivity descriptors. J. Phys. Chem. 106 (15), 3885–3890.

Parr, R.G., Yang, W.T., 1984. Density functional-approach to the frontier-electron theory of chemical-reactivity. J. Am. Chem. Soc. 106 (14), 4049–4050.

Pattison, D.I., Davies, M.J., 2001. Absolute rate constants for the reaction of hypochlorous acid with protein side chains and peptide bonds. Chem. Res. Toxicol. 14 (10), 1453–1464.

Pattison, D.I., Davies, M.J., 2004. Kinetic analysis of the reactions of hypobromous acid with protein components: implications for cellular damage and use of 3-bromotyrosine as a marker of oxidative stress. Biochemistry 43 (16), 4799–4809.

Penn, R.E., Block, E., Revelle, L.K., 1978. Flash vacuum pyrolysis studies. 5. Methanesulfenic acid. J. Am. Chem. Soc. 100 (11), 3622–3623.

Pryor, W.A., Giamalva, D.H., Church, D.F., 1984. Kinetics of ozonation .2. Amino-acids and model compounds in water and comparisons to rates in nonpolar-solvents. J. Am. Chem. Soc. 106 (23), 7094–7100.

Raghavachari, K., 2000. Perspective on "density functional thermochemistry. III. The role of exact exchange". Theo. Chem. Acc. 103 (3–4), 361–363.

Rehder, D.S., Borges, C.R., 2010. Cysteine sulfenic acid as an intermediate in disulfide bond formation and nonenzymatic protein folding. Biochemistry 49 (35), 7748–7755.

Rodgers, S.L., Cash, J.N., Siddiq, M., Ryser, E.T., 2004. A comparison of different chemical sanitizers for inactivating Escherichia coli O157:H7 and Listeria monocytogenes in solution and on apples, lettuce, strawberries, and cantaloupe. J. Food Protect. 67 (4), 721–731.

Rossoni, E.M.M., Gaylarde, C.C., 2000. Comparison of sodium hypochlorite and peracetic acid as sanitising agents for stainless steel food processing surfaces using epifluorescence microscopy. Int. J. Food Microbiol. 61 (1), 81–85.

Salgot, M., Folch, M., Huertas, E., Tapias, J., Avellaneda, D., Girós, G., Brissaud, F., Vergés, C., Molina, J., Pigem, J., 2002. Comparison of different advanced disinfection systems for wastewater reclamation. Water Sci. Technol. Water Supply 2 (3), 213–218.

Schnitzer, M., Hindle, D.A., 1980. Effect of peracetic-acid oxidation on N-containing components of humic materials. Can. J. Soil Sci. 60 (3), 541–548.

Shah, D.A., Liu, Z.-Q., Salhi, E., Hofer, T., von Gunten, U., 2015. Peracetic acid oxidation of saline waters in the absence and presence of H2O2: secondary oxidant and disinfection byproduct formation. Environ. Sci. Technol. 49, 1698–1705.

Shringarpure, R., Davies, K.J.A., 2002. Protein turnover by the proteasome in aging and disease. Free Radical Biol. Med. 32 (11), 1084–1089.

Stadtman, E.R., Van Remmen, H., Richardson, A., Wehr, N.B., Levine, R.L., 2005. Methionine oxidation and aging. Biochim. Biophys. Acta Protein Proteonomics 1703 (2), 135–140.

Tomita, M., Irie, M., Ukita, T., 1969. Sensitized photooxidation of histidine and its derivatives. Products and mechanism of the reaction. Biochemistry 8 (12), 5149–5160.

Trehy, M.L., Yost, R.A., Miles, C.J., 1986. Chlorination byproducts of amino acids in natural waters. Environ. Sci. Technol. 20 (11), 1117–1122.

Veschetti, E., Cutilli, D., Bonadonna, L., Briancesco, R., Martini, C., Cecchini, G., Anastasi, P., Ottaviani, M., 2003. Pilot-plant comparative study of peracetic acid and sodium hypochlorite wastewater disinfection. Water Res. 37 (1), 78–94.

Voukkali, I., Zorpas, A.A., 2015. Disinfection methods and by-products formation. Desalination Water Treat. 56 (5), 1150–1161.

Wenk, J., Aeschbacher, M., Salhi, E., Canonica, S., von Gunten, U., Sander, M., 2013. Chemical oxidation of dissolved organic matter by chlorine dioxide, chlorine, and ozone: effects on its optical and antioxidant properties. Environ. Sci. Technol. 47 (19), 11147–11156.

Wu, G., 2009. Amino acids: metabolism, functions, and nutrition. Amino Acids 37 (1), 1–17.

Zhang, K., Zhou, X., Du, P., Zhang, T., Cai, M., Sun, P., Huang, C.-H., 2017. Oxidation of β-lactam antibiotics by peracetic acid: reaction kinetics, product and pathway evaluation. Water Res. 123, 153–161.

Supporting Information

Oxidation of Amino Acids by Peracetic Acid: Reaction Kinetics, Pathways and Theoretical Calculations

Penghui Du[a,b,d], Wen Liu[b,c], Hongbin Cao[a], He Zhao[a], Ching-Hua Huang[b*]

[a] *Beijing Engineering Research Center of Process Pollution Control, Division of Environment Technology and Engineering, Institute of Process Engineering, Chinese Academy of Sciences, Beijing 100190, China*

[b] *School of Civil and Environmental Engineering, Georgia Institute of Technology, Atlanta, Georgia 30332, United States*

[c] *The Key Laboratory of Water and Sediment Sciences, Ministry of Education, College of Environmental Science and Engineering, Peking University, Beijing 100871, China*

[d] *University of Chinese Academy of Sciences, Beijing 100049, China*

* Corresponding author.

Tel: +1 4048947694; Email address: ching-hua.huang@ce.gatech.edu (C.-H. Huang).

Text S1. Quantification of amino acids

Amino acids were derivatized following previous methods (Newton et al., 1981; Donzanti and Yamamoto, 1988) with modifications before analysis. CYS was derivatized with mBBr and subsequently analyzed by HPLC coupled to a fluorescence (FLR) detector. Stock solution of the mBBr (10 mM) was prepared in acetonitrile; this solution was stable for up to six months at -20 °C. The stock solution was diluted to 100 µM with borate buffer (0.1 M, pH 8.8) before using for the derivatization of CYS. The derivatization was performed in a HPLC vial insert with 150 µL CYS sample and 150 µL borate buffer containing the 100 µM mBBr. The mixture was vortexed for 30 seconds before analysis. FLR detection was operated at an excitation wavelength of 395 nm and an emission wavelength of 475 nm.

The other amino acids were derivatized with OPA, a fresh solution of 70 mg OPA, 1 mL methanol, and 95 mL of buffer (pH 10.5, 25 g/L boric acid, 0.2% 2-mercaptoethanol) was prepared, which was stable up to 1 week at 4 °C. The derivatization was performed in a HPLC vial with 100 µL amino acids sample and 200 µL OPA working solution. The mixture was agitated for 1 min before analysis. FLR detection was operated at an excitation wavelength of 340 nm and an emission wavelength of 455 nm.

Text S2. Condensed Fukui function method

Fukui function, an important concept in conceptual density functional theory, has been widely used in prediction of reactive sites of electrophilic, nucleophilic, and radical attacks (Parr and Yang, 1984). Fukui function is defined as:

$$f(r) = \left[\frac{\partial \rho(\mathrm{r})}{\partial N} \right]_V \tag{1}$$

where $\rho(r)$ is the electron density at a point r in space, N is total electron number in present system, and the constant term v in the partial derivative is external potential. In the condensed version of Fukui function, atomic population number is used to represent the amount of electron density distribution around an atom. The condensed Fukui function can be calculated as follows:

$$\text{Electrophilic attack: } f^-(r) = \rho_N(r) - \rho_{N-1}(r) \tag{2}$$

$$\text{Nucleophilic attack: } f^+(r) = \rho_{N+1}(r) - \rho_N(r) \tag{3}$$

$$\text{Radical attack: } f^0(r) = [f^+(r) + f^-(r)]/2 = [\rho_{N+1}(r) - \rho_{N-1}(r)]/2 \tag{4}$$

where q^k is the atom charge of atom k at corresponding state. The reactive sites usually have larger values of Fukui index than other regions. We calculated the condensed Fukui index (f^-) of amino acid molecules for electrophilic attacks, as PAA is a strong electrophile reagent which is more likely to attack sites that can readily lose electrons (De Vleeschouwer et al., 2007; Zhang et al., 2017). In this study, Natural Population Analysis (NPA) charge was used as it is considered to be one of the most suitable methods to calculate Fukui index (Olah et al., 2002). A color gradient for the set of Fukui values was generated using the conditional formatting tool in Microsoft Excel 2013.

Text S3. Local Nucleophilicity Index calculations

The local nucleophilicity index (N_k) is calculated based on the global nucleophilicity index (N), which was proposed as the inverse of electrophilicity index ($1/\omega$) (Chattaraj and Maiti, 2001). The global electrophilicity index ω was defined as follows (Parr et al. 1999):

$$\omega = \frac{\mu^2}{2\eta} \tag{5}$$

where μ is the electronic chemical potential (Parr et al., 1978) and η is the chemical hardness (Parr and Pearson, 1983). For an N-electron system with external potential $v(r)$ and total energy E, the electronic chemical potential μ, the negative of electronegativity χ, is defined as the partial derivative of the energy of the number of electrons at constant external potential and in the absence of a magnetic field:

$$\mu = -\chi = \left(\frac{\partial E}{\partial N}\right)_{v(r)} \approx -\frac{I+A}{2} \tag{6}$$

where I and A are the vertical ionization potential and electron affinity, respectively. These two quantities were calculated, again using the B3LYP method and 6-31G(d,p) as basis set. Meanwhile, the chemical hardness η was defined as differentiating the chemical potential to the number of electrons, again at constant external potential:

$$\eta = \left(\frac{\partial^2 E}{\partial N^2}\right)_{v(r)} \approx I - A \tag{7}$$
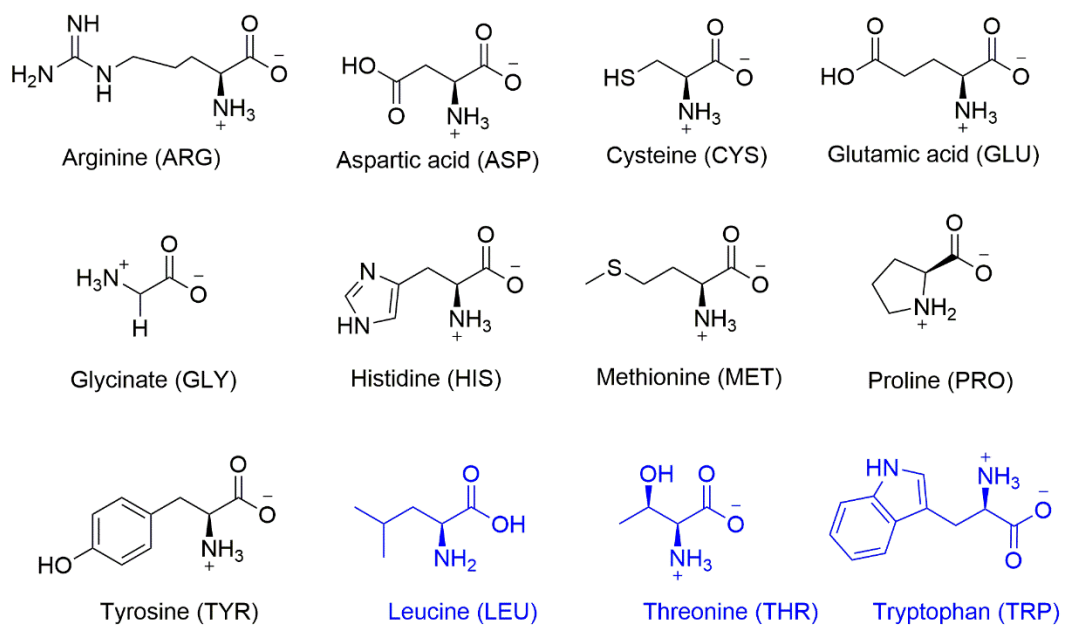
Figure S1. Structures of amino acids used in this work (Amino acids in blue were only used in theoretical prediction purpose).
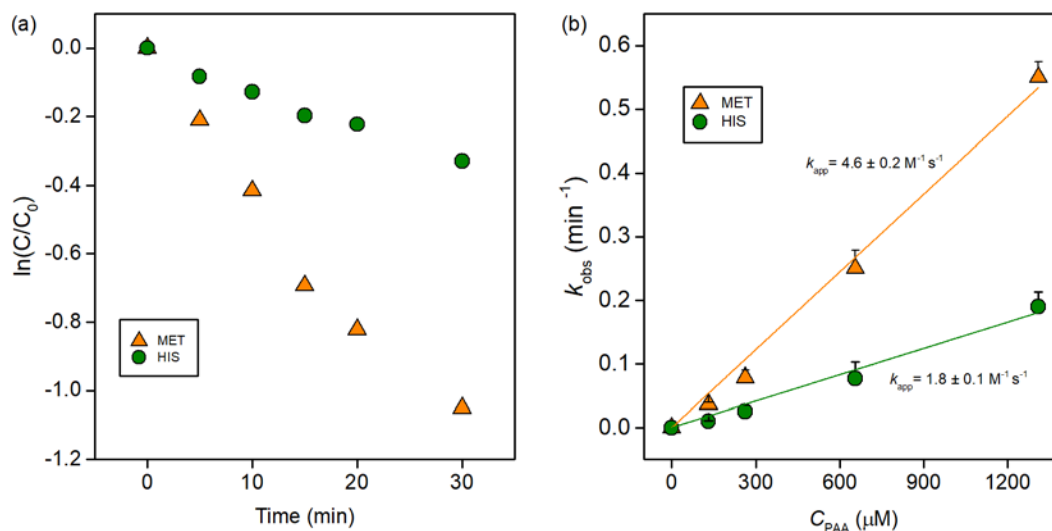
Figure S2. Degradation kinetics of MET and HIS by PAA solution. (a) $\ln(C/C_0)$ versus time, $[PAA]_0 = 131$ µM, (b) Relationship between the initial PAA concentration and pseudo-first-order rate constants for degradation of MET (orange triangles) and HIS (green circles). Solid lines represent linear regressions of second-order reaction kinetics with the fitting parameter k_{app}. Experimental conditions: [amino acids]$_0$ = 10 µM, $[PAA]_0$ = 131-1310 µM, pH = 7.0, room temperature).
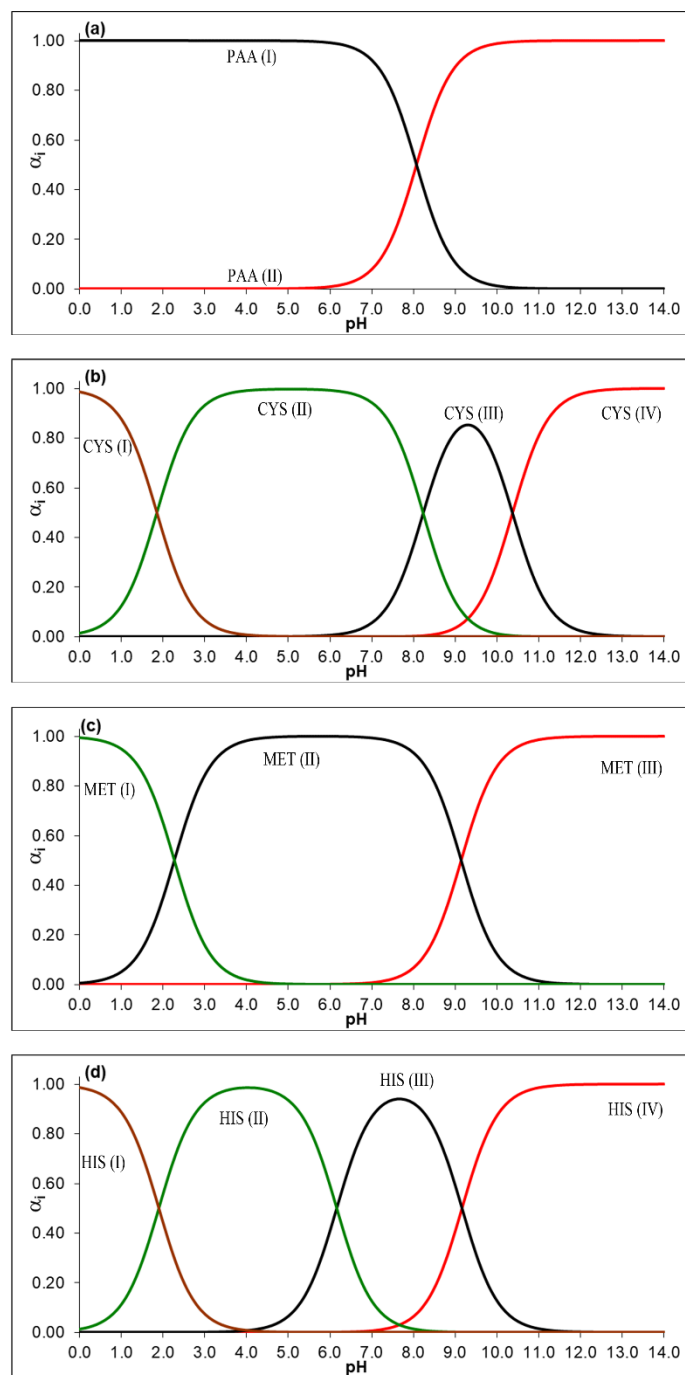
Figure S3. Acid-base speciation of PAA (a), CYS (b), MET (c), and HIS (d). α is the fraction of the PAA species.
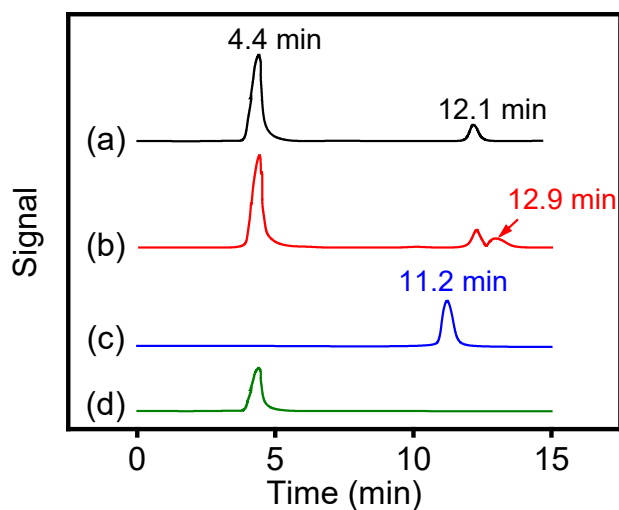
Figure S4. Ion chromatography of (a) 131 µM PAA solution, (b) 131 µM PAA+ 10 µM CYS solution (incubation 30 min), (c) 1 µM SO_4^{2-} solution, and (d) 1 µM acetic acid.

HOMO   LUMO
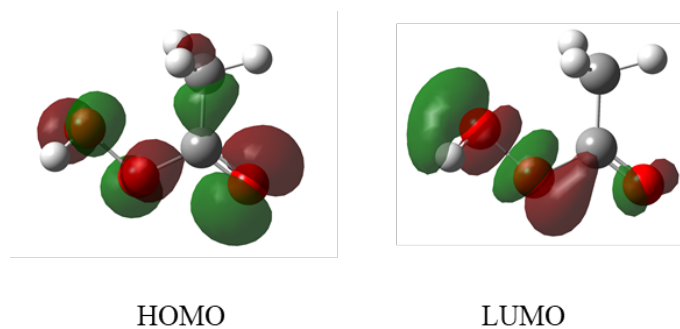
Figure S5. Molecular orbitals of PAA structure. (HOMO: Highest occupied molecular orbital; LUMO: Lowest unoccupied molecular orbital.)

Table S1. Species distribution (in fractions) of PAA and selected amino acids at pH 5, 7, and 9.
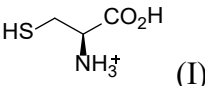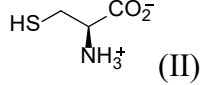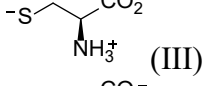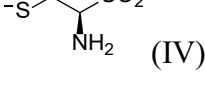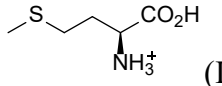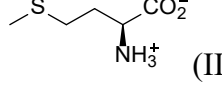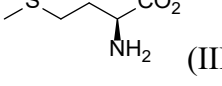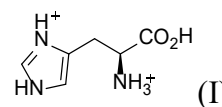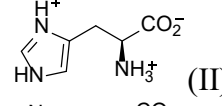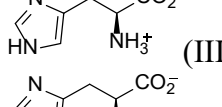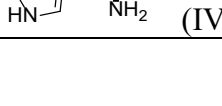
	Species	pH 5	pH 7	pH 9
PAA	$CH_3C(=O)OOH$ (I)	0.999	0.921	0.104
	$CH_3C(=O)OO^-$ (II)	0.001	0.079	0.896
CYS	HS–CH–CO_2H, NH_3^+ (I)	0.001	0.000	0.000
	HS–CH–CO_2^-, NH_3^+ (II)	0.998	0.944	0.139
	$^-$S–CH–CO_2^-, NH_3^+ (III)	0.000	0.056	0.826
	$^-$S–CH–CO_2^-, NH_2 (IV)	0.000	0.000	0.035
MET	S–CH–CO_2H, NH_3^+ (I)	0.002	0.000	0.000
	S–CH–CO_2^-, NH_3^+ (II)	0.998	0.993	0.577
	S–CH–CO_2^-, NH_2 (III)	0.000	0.007	0.423
HIS	imidazole-H^+–CH–CO_2H, NH_3^+ (I)	0.001	0.000	0.000
	imidazole-H^+–CH–CO_2^-, NH_3^+ (II)	0.934	0.124	0.001
	imidazole–CH–CO_2^-, NH_3^+ (III)	0.065	0.870	0.588
	imidazole–CH–CO_2^-, NH_2 (IV)	0.000	0.006	0.411

Table S2. Cartesian coordinate of ARG

Symbol	X	Y	Z
C	0.96854	0.68678	0.65422
C	2.18616	0.59161	-0.28343
N	3.23174	1.61061	-0.05742
C	2.86520	-0.79940	-0.24470
O	4.18714	-0.74964	-0.46047
O	2.26886	-1.83671	-0.06531
H	1.25583	0.31529	1.64762
H	1.84393	0.71872	-1.31964
H	4.39634	0.21444	-0.50545
H	2.98205	2.49430	-0.49123
H	0.72756	1.75214	0.77451
C	-0.27530	-0.05966	0.15582
H	-0.03288	-1.11279	0.00017
H	-0.58473	0.34950	-0.81425
C	-1.44996	0.05279	1.13716
H	-1.19131	-0.45149	2.07381
H	-1.63256	1.10927	1.39489
N	-2.66211	-0.57303	0.62687
H	-3.14555	-1.18479	1.26949
C	-3.50900	0.09299	-0.25528
N	-4.65707	-0.65679	-0.53639
H	-5.19728	-0.20920	-1.26644
H	-4.46656	-1.62884	-0.75103
N	-3.35594	1.24842	-0.79433
H	-2.55521	1.73956	-0.39920
H	3.34221	1.78954	0.93904

Table S3. Cartesian coordinate of ASP

Symbol	X	Y	Z
C	0.58472	0.97371	-0.49207
C	-0.71662	0.64179	0.25639
N	-1.84673	1.54386	-0.01496
C	-1.16386	-0.80913	-0.02247
O	-2.49152	-0.98109	0.03144
O	-0.38433	-1.70738	-0.23754
H	0.46148	0.85494	-1.57159
H	-0.51803	0.68369	1.33329
H	-2.86101	-0.07570	0.15215
H	-1.77657	2.40269	0.52196
H	0.83868	2.02373	-0.29780
C	1.79302	0.14843	-0.08953
O	2.64865	-0.24535	-0.84477
O	1.85603	-0.02403	1.25491
H	2.64649	-0.56499	1.41949
H	-1.87815	1.80258	-0.99899

Table S4. Cartesian coordinate of CYS

Symbol	X	Y	Z
C	0.76698	-0.58185	-0.42422
C	-0.23422	0.16341	0.47401
N	-0.14833	1.61597	0.28297
C	-1.64858	-0.32320	0.07824
O	-2.34424	0.57527	-0.63002
O	-2.05438	-1.42774	0.35299
H	0.59787	-0.31328	-1.47171
H	0.61018	-1.65615	-0.32271
H	-0.07366	-0.15355	1.51269
H	-1.75486	1.36785	-0.67337
H	-0.41540	2.10728	1.13183
S	2.53415	-0.16392	-0.11989
H	2.60032	-0.65768	1.13422
H	0.81141	1.88604	0.07456

Table S5. Cartesian coordinate of GLU

Symbol	X	Y	Z
C	1.16814	0.33917	-0.43143
N	1.46178	1.71492	0.00957
C	2.34164	-0.58213	-0.01432
O	3.45421	0.08531	0.31823
O	2.26464	-1.78826	-0.02187
H	1.18713	0.34254	-1.52973
H	3.20083	1.03758	0.26001
H	1.08622	2.41041	-0.62636
C	-0.17025	-0.24491	0.04105
H	-0.18621	-1.30453	-0.22763
H	-0.21794	-0.19790	1.13555
C	-1.38330	0.48276	-0.56173
H	-1.34251	1.54924	-0.30454
H	-1.39238	0.39756	-1.65142
C	-2.70781	-0.05536	-0.06500
O	-2.80865	0.03349	1.28635
H	-3.67606	-0.34019	1.51718

Table S6. Cartesian coordinate of GLY

Symbol	X	Y	Z
C	0.64106	-0.79643	0.10179
C	-0.69377	-0.03693	0.00422
O	-1.75955	-0.59783	-0.08210
O	-0.55236	1.29573	0.05320
H	0.60912	-1.62604	-0.61275
H	0.67677	-1.24063	1.10180
N	1.77586	0.12148	-0.07178
H	0.42283	1.44135	0.10566
H	2.55503	-0.11912	0.53132
H	2.11676	0.11101	-1.02838

Table S7. Cartesian coordinate of HIS

Symbol	X	Y	Z
C	-3.08107	0.82213	-0.00063
N	-1.80624	0.95313	0.29771
C	-1.27664	-0.32701	0.27297
C	-2.26126	-1.23036	-0.04620
N	-3.40971	-0.48286	-0.21647
C	0.17233	-0.57334	0.56419
C	1.13255	0.10750	-0.43810
N	1.04927	1.57562	-0.34530
C	2.57252	-0.34016	-0.10404
O	3.31906	0.63439	0.42942
O	2.96349	-1.47241	-0.27817
H	-3.80316	1.62356	-0.07006
H	-2.24973	-2.30297	-0.16063
H	-4.32445	-0.83947	-0.44652
H	0.41343	-0.20408	1.56974
H	0.38569	-1.64502	0.55252
H	0.90733	-0.27390	-1.44226
H	2.70974	1.41888	0.43394
H	0.11892	1.85433	-0.03013
H	1.19802	1.99907	-1.25730

Table S8. Cartesian coordinate of MET

Symbol	X	Y	Z
C	-0.04311	-0.36915	-0.14744
C	-1.29313	0.37390	0.34698
N	-1.50613	1.72302	-0.21079
C	-2.56775	-0.47256	0.10506
O	-3.64361	0.26047	-0.21161
O	-2.59281	-1.67467	0.22620
H	-0.07075	-0.42071	-1.24421
H	-0.09883	-1.39944	0.21353
H	-1.23173	0.48475	1.43830
H	-3.30663	1.18697	-0.26500
H	-1.01160	2.43469	0.31684
C	1.25848	0.29110	0.31064
H	1.30091	1.33699	-0.01684
H	1.32598	0.27735	1.40521
S	2.70212	-0.60040	-0.38897
C	4.05224	0.40821	0.31319
H	4.98920	-0.02841	-0.03876
H	3.99635	1.44441	-0.03174
H	4.04106	0.38111	1.40617
H	-1.17399	1.77205	-1.17187

Table S9. Cartesian coordinate of PRO

Symbol	X	Y	Z
C	-1.46654	-0.01682	0.00186
O	-1.57654	-1.20116	-0.61125
O	-2.31907	0.84096	-0.02576
C	-0.13073	0.16533	0.75828
C	0.68202	1.35078	0.19313
H	-0.39068	0.32372	1.81017
C	1.99425	-0.63390	-0.08086
C	1.63481	0.66992	-0.80216
H	1.25418	1.82682	0.99683
H	0.03093	2.10522	-0.25202
H	2.78510	-0.45049	0.66101
H	2.34554	-1.41853	-0.75827
H	2.51556	1.27148	-1.04058
H	1.11339	0.45027	-1.74071
N	0.72259	-1.03708	0.56732
H	0.88111	-1.53403	1.43708
H	-0.71114	-1.64513	-0.41007

Table S10. Cartesian coordinate of TYR

Symbol	X	Y	Z
C	0.92879	-0.24847	0.80814
C	1.81868	-0.09980	-0.45030
N	1.65469	1.22974	-1.06017
C	3.28968	-0.28554	-0.02657
O	3.98921	0.85844	0.00461
O	3.74744	-1.35978	0.28660
H	1.20718	0.53605	1.52187
H	1.18787	-1.20677	1.26822
H	1.58099	-0.92075	-1.13838
H	3.35159	1.54380	-0.31276
H	1.80370	1.18681	-2.06488
C	-0.55229	-0.17406	0.50965
C	-1.29855	0.97265	0.80456
C	-1.22109	-1.25157	-0.09532
C	-2.66083	1.05253	0.50607
H	-0.81527	1.81616	1.29195
C	-2.57567	-1.18923	-0.39787
H	-0.67041	-2.16034	-0.32575
C	-3.30352	-0.03016	-0.09836
H	-3.22070	1.95258	0.75111
H	-3.09016	-2.02596	-0.85845
O	-4.63135	-0.02379	-0.41697
H	-5.01935	0.81946	-0.14855
H	0.70812	1.57373	-0.91709

Table S11. Cartesian coordinate of TRP

Symbol	X	Y	Z
C	-1.19630	0.31776	-0.86452
C	-1.96743	-0.18716	0.38297
N	-2.08077	0.87918	1.39034
C	-3.37732	-0.61743	-0.06408
O	-4.34003	0.24849	0.28709
O	-3.58116	-1.62041	-0.70814
H	-1.74638	1.16695	-1.28802
H	-1.23025	-0.48483	-1.60825
H	-1.46373	-1.08420	0.76265
H	-2.10088	0.48852	2.32869
H	-1.26619	1.48819	1.34182
C	0.21711	0.72438	-0.57122
C	1.32759	-0.14410	-0.25286
C	0.70947	2.00773	-0.53520
C	2.46229	0.68483	-0.03759
N	2.05374	1.99162	-0.21436
H	0.20396	2.94157	-0.74020
H	2.64762	2.80233	-0.15752
C	3.83116	-1.21760	0.39311
C	2.72132	-2.06045	0.17902
C	1.47518	-1.53834	-0.14205
C	3.71914	0.16343	0.28683
H	4.79278	-1.65584	0.64261
H	2.84720	-3.13541	0.26513
H	0.62994	-2.19922	-0.31214
H	4.57597	0.81144	0.44771
H	-3.86448	0.94197	0.80758

Table S12. Cartesian coordinate of LEU

Symbol	X	Y	Z
C	0.50611	0.89877	-0.14291
C	-0.80308	0.49432	0.56962
N	-1.77062	1.60621	0.47373
C	-1.42553	-0.74782	-0.09882
O	-2.42927	-0.45946	-0.94005
O	-1.02395	-1.87333	0.09403
H	0.24546	1.22798	-1.15796
H	-0.58044	0.21562	1.60578
H	-2.56368	0.51420	-0.83483
H	-2.38866	1.62682	1.28050
H	0.89945	1.78262	0.38207
C	1.62071	-0.16253	-0.22515
H	1.23136	-1.01751	-0.78973
H	-1.29692	2.50396	0.43186
C	2.81820	0.41488	-0.99456
H	3.25940	1.26652	-0.46167
H	3.60213	-0.33922	-1.11765
H	2.52812	0.76048	-1.99300
C	2.04833	-0.67761	1.15652
H	2.35449	0.14690	1.81347
H	1.24004	-1.23126	1.64066
H	2.90096	-1.35834	1.06435

Table S13. Cartesian coordinate of THR

Symbol	X	Y	Z
C	1.11996	-0.15468	-0.35000
C	-0.06111	0.36830	0.49793
N	-0.22060	1.81479	0.27340
C	-1.36522	-0.34301	0.07168
O	-2.15229	0.42198	-0.69456
O	-1.63286	-1.48367	0.37486
H	0.84182	-0.04712	-1.41142
H	0.13206	0.10848	1.54636
H	-1.68260	1.29505	-0.72612
H	-0.58055	2.26765	1.10910
H	0.69365	2.21724	0.07904
C	1.47872	-1.60633	-0.05199
H	0.62007	-2.26331	-0.20185
H	2.29164	-1.93693	-0.70851
H	1.81415	-1.70302	0.98504
O	2.21300	0.72427	-0.05241
H	2.95706	0.47208	-0.61429

References

Chattaraj, P., Maiti, B., 2001. Reactivity dynamics in atom− field interactions: A quantum fluid density functional study. J. Phys. Chem. A 105 (1), 169-183.

De Vleeschouwer, F., Van Speybroeck, V., Waroquier, M., Geerlings, P., De Proft, F., 2007. Electrophilicity and nucleophilicity index for radicals. Org. Lett. 9 (14), 2721-2724.

Donzanti, B.A., Yamamoto, B.K., 1988. An improved and rapid HPLC-EC method for the isocratic separation of amino acid neurotransmitters from brain tissue and microdialysis perfusates. Life Sci. 43 (11), 913-922.

Newton, G.L., Dorian, R., Fahey, R.C., 1981. Analysis of biological thiols: Derivatization with monobromobimane and separation by reverse-phase high-performance liquid chromatography. Anal. Biochem. 114 (2), 383-387.

Olah, J., Van Alsenoy, C., Sannigrahi, A.B., 2002. Condensed fukui functions derived from stockholder charges: Assessment of their performance as local reactivity descriptors. J. Phys. Chem. A 106 (15), 3885-3890.

Parr, R.G., Donnelly, R.A., Levy, M., Palke, W.E., 1978. Electronegativity: The density functional viewpoint. J. Chem. Phys. 68 (8), 3801-3807.

Parr, R.G., Pearson, R.G., 1983. Absolute hardness: Companion parameter to absolute electronegativity. J. Am. Chem. Soc. 105 (26), 7512-7516.

Parr, R.G., Szentpály, L.V., Liu, S., 1999. Electrophilicity index. J. Am. Chem. Soc. 121 (9), 1922-1924.

Parr, R.G., Yang, W.T., 1984. Density functional-approach to the frontier-electron theory of chemical-reactivity. J. Am. Chem. Soc. 106 (14), 4049-4050.

Zhang, K., Zhou, X., Du, P., Zhang, T., Cai, M., Sun, P., Huang, C.-H., 2017. Oxidation of β-lactam antibiotics by peracetic acid: Reaction kinetics, product and pathway evaluation. Water Res. 123, 153-161.